Author 1:
Surname: Câmpian
First Name: Marius V.
Corresponding: no
E-Mail: no
Affiliation: Department of Chemistry, Babes-Bolyai University, Cluj-Napoca, RO-400028, Romania

Author 2:
Surname: Azizuddin
First Name: Aliaa Diyana
Corresponding: no
E-Mail: no
Affiliation: Department of Chemistry, University of Malaya, 50603 Kuala Lumpur, Malaysia

Author 3:

Surname: Haiduc

First Name: Ionel

Corresponding: no

E-Mail: no

Affiliation: Department of Chemistry, Babes-Bolyai University, Cluj-Napoca, RO-400028, Romania

Author 4:

Surname: Tiekink

First Name: Edward R.T.

Corresponding: yes

E-Mail: edwardt@sunway.edu.my

Affiliation: Research Centre for Crystalline Materials, Faculty of Science and Technology, Sunway University, 47500 Bandar Sunway, Selangor Darul Ehsan, Malaysia

Data checked and receipted   **Date:**

Wenn Sie die Korrektheit der Daten nicht durch einen Haken bestätigen oder keine Änderungen in diesem Formular angeben, gehen wir davon aus, dass die angegebenen Daten korrekt sind.

If you don't confirm the correctness by checking the box or implement your corrections in this form, we have to presume that all data are correct.

Marius V. Câmpian, Aliaa Diyana Azizuddin, Ionel Haiduc and Edward R.T. Tiekink*

Mono urotropine adducts of some binary zinc xanthates and dithiocarbamates: solid-state molecular structures and supramolecular self-assembly

Abstract: The molecular structures of [Zn(S$_2$COR)$_2$(hmta)], R = Et (**I**) and iPr (**II**), and [Zn(S$_2$CNRR′)$_2$(hmta)], R = R′ = Et (**III**) and R = iPr, R′ = CH$_2$CH$_2$OH (**IV**), feature chelating 1,1-dithiolate ligands and monodentate hmta molecules; hmta = hexamethylenetetramine. The resulting NS$_4$ donor sets are highly distorted, with tendencies towards square pyramidal. Systematic differences in the structures are related to the greater chelating ability of the dithiocarbamate ligands leading to, e.g., elongated Zn–N bond lengths in **III** and **IV**. In the molecular packing, an unusual C–H···π(chelate ring) interaction is noted in **III**, which is correlated with the close to symmetric Zn–S bond lengths formed by the relevant dithiocarbamate ligand and resultant greater metalloaromatic character of the resulting ZnS$_2$C chelate ring, and to the greater distortion of the coordination geometry compared with literature precedents. A three-dimensional architecture found for **IV** is sustained by hydroxyl-O-H···O, S and N hydrogen bonding.

Keywords: crystal structure analysis; dithiocarbamate; urotropine; X-ray diffraction; zinc.

Introduction

1,3,5,7-Tetraazatricyclo[3.3.1.1^{3,7}]decane, more commonly referred to as urotropine or hexamethylenetetramine (hmta), is reported as the first crystal structure of an organic molecule described in the open literature [1].

*Corresponding author: Edward R.T. Tiekink, Research Centre for Crystalline Materials, Faculty of Science and Technology, Sunway University, 47500 Bandar Sunway, Selangor Darul Ehsan, Malaysia, E-mail: edwardt@sunway.edu.my
Marius V. Câmpian and Ionel Haiduc: Department of Chemistry, Babes-Bolyai University, Cluj-Napoca, RO-400028, Romania
Aliaa Diyana Azizuddin: Department of Chemistry, University of Malaya, 50603 Kuala Lumpur, Malaysia

Aesthetically attractive and of high symmetry, this cage-like structure has four tertiary-amine atoms interlinked by methylene groups; however, the compact cage cavity is too small to accommodate other species. With four potential donor atoms for metals, it is not surprising that this molecule has long attracted the attention of coordination chemists, in particular in the context of constructing metal-organic frameworks (MOFs) [2–4]. While not as well studied as poly-pyridyl linkers in the constructions of MOF's, μ$_2$-, μ$_3$- and μ$_4$-coordination modes of hmta have been revealed by crystallography. A search of the most recent version of the Cambridge Structural Database [5] reveals no less than 700 "hits" of which well over half contain a coordinated transition metal. All this interest notwithstanding, the coordination chemistry of hmta with metal 1,1-dithiolates, e.g. dithiocarbamates, xanthates and dithiophosphates, is comparatively rare [6]. While a summary of relevant structures is given below, it is salient to highlight some recent results in the structural chemistry of cadmium xanthate adducts of hmta as these motivated the present study.

In earlier work, reactions between Cd(S$_2$COR)$_2$ for R = Me, Et and iPr, with hmta gave only three products despite varying the ratios between reactants, i.e. 1:2, 1:1 and 2:1 [6]. The isolated structures were also of interest as the compositions were very distinct. Thus, for R = Me, a 1:1 adduct was isolated and a one-dimensional coordination polymer was formed as hmta was μ$_2$-bridging. A one-dimensional polymer was also formed by the R = Et compound but the stoichiometry of the adduct was 2:1 with the key difference being that the hmta ligand was μ$_3$-bridging, linking two Cd(S$_2$COEt)$_2$ entities in the chain as well as a terminal Cd(S$_2$COEt)$_2$ residue. In contrast, a zero-dimensional species was formed when R = iPr in the 1:1 adduct with hmta μ$_2$-bridging. In keeping with the notion that steric effects are crucial in determining supramolecular aggregation in main group element 1,1-dithiolates [7, 8], steric reasons were proffered to explain the different solid-state structures. The zero-dimensional adduct is clearly correlated with the presence of the relatively large iso-propyl substituent. Similarly, a more open arrangement

was found in the one-dimensional polymer for the R = Et compared with R = Me and this enabled the attachment of the pendant Cd(S$_2$COEt)$_2$ residue. With this background in mind, it was thought of interest to continue these studies with binary zinc xanthates which resulted in the characterisation of **I** and **II**, Figure 1. In addition, studies were performed with related zinc dithiocarbamates leading to **III** and **IV**, Figure 1, as these have proven to provide interesting supramolecular chemistry owing to their potential for forming hydrogen bonding interactions [9–12]. Herein, the crystal and molecular structures of **I**–**IV** are described.

Experimental

Instrumentation

All chemicals and solvents were used as purchased without purification. The reactions were carried out under ambient conditions. Elemental analyses were performed on a Perkin Elmer PE 2400 CHN Elemental Analyser. Melting points were determined on a Krüss KSP1N melting point meter. ^{1}H NMR spectra were recorded in CDCl$_3$ (298 K) on a Bruker Avance 300 spectrometer for **I**, and in d_6-DMSO solutions (298 K) on a Bruker Avance 400 MHz NMR spectrometer for **II**–**IV**; cited chemical shifts are relative to CHCl$_3$ and tetramethylsilane, respectively; abbreviations for NMR assignments: s, singlet;

Fig. 1: Chemical diagrams of the two zinc xanthate/hmta, (**I**) and (**II**), and two zinc dithiocarbamate/hmta, (**III**) and (**IV**), compounds investigated herein.

d, doublet; t, triplet; q, quartet; $sept$, septet; m, multiplet; br, broad. IR spectra were obtained on a Perkin Elmer Spectrum 400 FT Mid-IR/Far-IR spectrophotometer from 4000 to 400 cm^{-1}; abbreviations: vs, very strong; s, strong; m, medium; br, broad.

Synthesis and characterisation

Synthesis of binary zinc xanthate and dithiocarbamate precursors: Zn(S$_2$COR)$_2$ for R = Et and iPr, were obtained from the reaction of xanthate salt (synthesised by the reaction of one mole of the respective alcohol with two mole equivalents of CS$_2$ in the presence of base) and Zn(NO$_3$)$_2$·6H$_2$O in aqueous solution to yield a white powder.

Zn(S$_2$CNRR′)$_2$ for R = R′ = Et$_2$, and R = iPr, R′ = CH$_2$CH$_2$OH, were obtained from the reaction of dithiocarbamate salt (synthesised by the reaction of one mole of the respective amine with two mole equivalents of CS$_2$ in the presence of base) and Zn(NO$_3$)$_2$·6H$_2$O in aqueous solution to yield a white powder.

Synthesis of (I)–(IV): Each of the Zn(S$_2$COR′)$_2$ and Zn(S$_2$CNRR′)$_2$ precursors was dissolved in a solvent mixture of 3MeOH/acetonitrile, together with hexamethylenetetramine (hmta; Acros Organic). The resulting mixture was stirred for 5 h at 333 K and left for slow evaporation at room temperature. This procedure yielded crystals after 3 weeks in cases of **II**–**IV**. In the case of **I**, the powder was filtered off and crystals obtained by layering hexane over a solution of **I** in CHCl$_3$. Using these procedures the following compounds were prepared:

Zn(S$_2$COEt)$_2$(hmta) (I)
^{1}H NMR: δ 4.91 (s, 12H, CH$_2$), 4.49 (q, 4H, OCH$_2$, J = 7 Hz), 1.44 (t, 6H, CH$_3$, J = 7 Hz) ppm. IR (cm^{-1}): 1205 (vs) ν(C–O), 1047 (vs) ν(C–S). M.pt: 389–390 K.

Zn(S$_2$COiPr)$_2$(hmta) (II)
Anal. Calc. for C$_{14}$H$_{26}$N$_4$O$_2$S$_4$Zn: C, 35.3; H, 5.5; N, 11.8. Found: C, 35.0; H, 5.3; N, 11.7. ^{1}H NMR: δ 5.32 ($sept$, 2H, OCH, J = 6.20 Hz), 4.60 (s, 12H, CH$_2$), 1.29 (d, 12H, CH$_3$, J = 6.20 Hz) ppm. IR (cm^{-1}): 1203 (vs) ν(C–O), 1017 (vs) ν(C–S). M.pt: 430 K.

Zn(S$_2$CNEt$_2$)$_2$(hmta) (III)
Anal. Calc. for C$_{16}$H$_{32}$N$_6$S$_4$Zn: C, 38.3; H, 6.4; N, 16.7. Found: C, 38.25; H, 6.60; N, 16.54. ^{1}H NMR: δ 4.67 (s, 12H, CH$_2$), 3.82 (q, 8H, NCH$_2$, J = 7.04 Hz), 1.22 (t, 12H, CH$_3$, J = 7.06 Hz) ppm. IR (cm^{-1}): 1440 (m) ν(C-N), 1047 (w), 998 (vs) ν(C–S). M.pt: 436 K.

Zn[S$_2$CN(iPr)CH$_2$CH$_2$OH]$_2$(hmta) (IV)
Anal. Calc. for C$_{18}$H$_{36}$N$_6$O$_2$S$_4$Zn: C, 38.5; H, 6.5; N, 15.0. Found: C, 38.37; H, 6.51; N, 14.68. ^{1}H NMR: δ 5.14 ($sept$, 2H, OCH, J = 6.59 Hz), 4.85 (br, s, 2H, OH), 4.62 (s, 12H, CH$_2$), 3.74–3.67 (m, 8H, CH$_2$CH$_2$), 1.18 (d, 12H, CH$_3$, J = 6.68 Hz) ppm. IR (cm^{-1}): 1448 (m) ν(C-N), 1022 (s), 992 (s) ν(C–S). M.pt: 428 K.
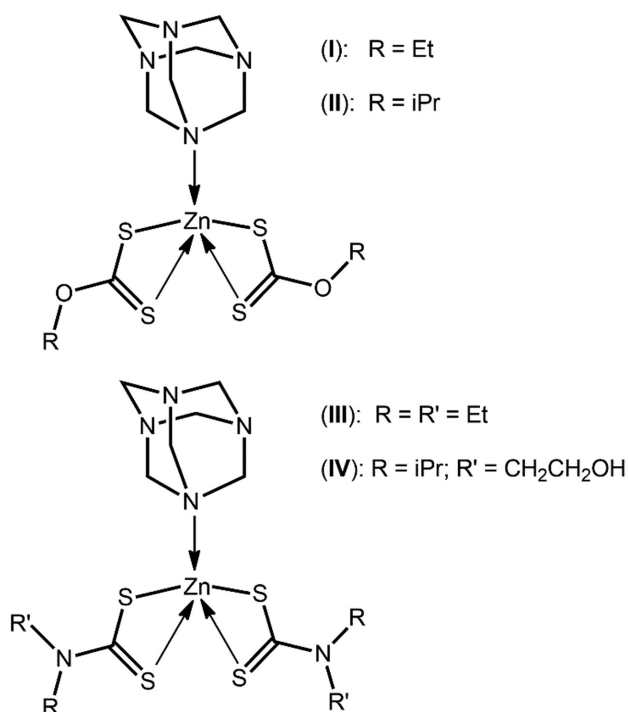
Crystal structure determination

A Rigaku AFC12κ/SATURN724 diffractometer fitted with Mo Kα radiation (λ = 0.71073 Å) was employed to measure intensity data for colourless **I** at 98 K. Data processing and absorption corrections

were accomplished with CrystalClear [13] and ABSCOR [14], respectively. Intensity data for colourless **II–IV** were measured at 100 K on an Agilent Technologies SuperNova Dual CCD with an Atlas detector also fitted with Mo Kα radiation. Data processing and absorption correction were accomplished with CrysAlis PRO [15]; numerical (gaussian) corrections were applied in the cases of **III** and **IV**. With the use of SHELXS-97 [16] and SHELXL-2014/7 [17] programmes integrated into WinGX [18], the structures were solved by direct methods and refined on F^2 by full-matrix least-squares with anisotropic displacement parameters for all non-hydrogen atoms. The C-bound H atoms were placed on stereochemical grounds and refined in the riding model approximation with $U_{iso} = 1.2–1.5U_{eq}$(carrier atom). The O-bound H atoms in **IV** were located from a difference map and refined with O–H = 0.84 ± 0.01 Å, and with $1.5U_{eq}$(O). A weighting scheme of the form $w = 1/[\sigma^2(F_o^2) + (aP)^2 + bP]$ where $P = (F_o^2 + 2F_c^2)/3$ was introduced in each case. For **II**, owing to poor agreement, perhaps due to the effect of the beam-stop, a low angle reflection, i.e. (0 1 1) was omitted from the final refinement. For **III**, three reflections were omitted, i.e. (0 – 1 1), (0 1 0) and (7 – 7 9), and for **IV**, four were omitted, i.e. (0 – 3 2), (0 1 2), (0 – 3 1) and (0 2 0). In **I**, the maximum and minimum residual electron density peaks of 1.40 and 0.81 Å^{-3}, respectively, were located 0.88 and 0.91 Å from the S2 and Zn atoms, respectively. For **III**, these were 0.71 and 1.53 Å^{-3}, respectively, and were located 0.89 and 0.95 Å from the Zn atom. Unit cell data, X-ray data collection parameters, and details of the

structure refinement are given in Table 1. The programmes ORTEP-3 for Windows [18], PLATON [19], DIAMOND [20] and QMol [21] were also used in the analysis.

Results

General

The 1:1 reactions between the selected binary zinc xanthates and dithiocarbamates and hmta afforded **I–IV** in good yields. The spectroscopy (^{1}H NMR and IR) showed the expected features and confirmed the 1:1 stoichiometries. Unambiguous structure determination was afforded by single crystal X-ray crystallography.

Crystal and molecular structures

The molecular structure of [Zn(S$_2$COMe)$_2$(hmta)], (**I**), is shown in Figure 1 and selected geometric parameters are

**Tab. 1:** Crystallographic data and refinement details for **I–IV**.[a]

	I	II	III	IV
Formula	$C_{12}H_{22}N_4O_2S_4Zn$	$C_{14}H_{26}N_4O_2S_4Zn$	$C_{16}H_{32}N_6S_4Zn$	$C_{18}H_{36}N_6O_2S_4Zn$
Formula weight	447.94	476.00	502.08	562.14
Crystal size (mm)	$0.08 \times 0.13 \times 0.29$	$0.15 \times 0.20 \times 0.25$	$0.10 \times 0.17 \times 0.28$	$0.23 \times 0.25 \times 0.35$
Crystal system	Monoclinic	Monoclinic	Triclinic	Triclinic
Space group	$C2/c$	$P2_1/n$	$P\bar{1}$	$P\bar{1}$
a/Å	21.052(5)	11.2276(6)	9.1148(5)	8.91570(10)
b/Å	9.0532(18)	10.8377(5)	10.8668(8)	23.0900(4)
c/Å	21.590(5)	17.0300(9)	12.6688(9)	25.7813(5)
α/°	90	90	103.797(6)	108.000(2)
β/°	107.363(4)	103.340(6)	94.841(5)	99.3610(10)
γ/°	90	90	114.026(6)	90.6930(10)
V/Å^3	3927.4(15)	2016.32(18)	1089.49(14)	4969.44(15)
Z/Z'	8/1	4/1	2/1	8/4
D_c/g cm^{-3}	1.515	1.568	1.530	1.503
μ/mm^{-1}	1.687	1.648	1.525	1.352
θ range/°	2.8–25.0	2.5–27.5	2.5–27.5	1.4–27.5
Reflections measured	11154	17547	10430	64129
Independent reflections; R_{int}	3441; 0.044	4635; 0.048	4982; 0.047	22852; 0.046
Reflections with $I > 2\sigma(I)$	3146	3759	4186	17154
Number of parameters	210	230	248	1157
R, obs. data; all data	0.068; 0.073	0.033; 0.048	0.042; 0.053	0.043; 0.066
a; b in wght scheme	0.074; 27.714	0.024; 0.631	0.055; 0.034	0.040; – 4.614
R_w, obs. data; all data	0.167; 0.171	0.064; 0.072	0.101; 0.111	0.093; 0.108
GoF (F^2)	1.07	1.05	1.07	1.07
$\Delta\rho_{max, min}$ (e Å^{-3})	1.40, – 0.81	0.45, – 0.36	0.71, – 1.53	0.84; – 0.66

[a]Supplementary material: Crystallographic data (excluding structure factors) for the structures reported in this paper have been deposited with the Cambridge Crystallographic Data Centre as supplementary publications no. CCDC-1409583-1409586. Copies of available material can be obtained free of charge, on application to CCDC, 12 Union Road, Cambridge CB2 1EZ, UK, (fax: +44-(0)1223-336033 or e-mail: deposit@ccdc.cam.ac.uk). The list of Fo/Fc-data is available from the author up to 1 year after the publication has appeared.

Tab. 2: Selected geometric parameters (Å, °) for **I** and **II**.

|	**I (n = 4)**	**II (n = 5)**
Zn–S1	2.2995(15)	2.3127(6)
Zn–S2	2.802(2)	2.8753(6)
Zn–S3	2.3452(14)	2.3732(7)
Zn–S4	2.5712(17)	2.4696(6)
Zn–N1	2.056(4)	2.0591(19)
C1–S1	1.691(8)	1.720(2)
C1–S2	1.657(7)	1.678(2)
C1–O1	1.369(7)	1.326(3)
C(n)–S3	1.715(6)	1.714(2)
C(n)–S4	1.677(5)	1.697(2)
C(n)–O2	1.330(6)	1.314(3)
S1–Zn–S2	69.86(6)	69.020(19)
S1–Zn–S3	130.44(6)	120.80(2)
S1–Zn–S4	101.52(6)	107.30(2)
S1–Zn–N1	119.41(11)	124.26(5)
S2–Zn–S3	94.89(6)	88.84(2)
S2–Zn–S4	156.54(6)	158.90(2)
S2–Zn–N1	98.68(13)	93.81(5)
S3–Zn–S4	73.78(5)	75.13(2)
S3–Zn–N1	109.21(11)	110.87(5)
S4–Zn–N1	104.42(13)	104.59(5)

included in Table 2. The zinc atom is chelated by two xanthate ligands with the final position in the penta-coordinated geometry occupied by a nitrogen donor from the hmta ligand. The xanthate ligands coordinate in an asymmetric fashion with the difference between the Zn–S_{short} and Zn–S_{long} bonds, ΔS, being 0.50 Å for the S1-containing xanthate ligand. The Zn–S bonds for the S3-xanthate fall within the range of bond lengths formed by the S1-xanthate so that ΔS is reduced to 0.22 Å. Based on a value of τ of 0.43 [22], the NS_4 donor set defines a coordination geometry intermediate between a square pyramidal ($\tau = 0.0$) and trigonal bipyramidal ($\tau = 1.0$) with a slight tendency
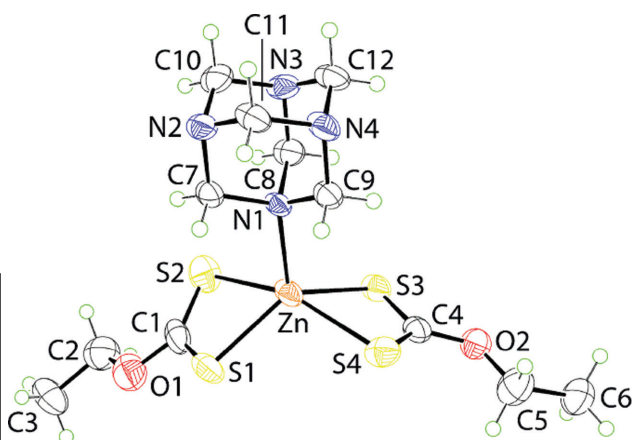
Fig. 2: The molecular structure of **I**, showing atom-labelling and displacements ellipsoids at the 50% probability level.

towards the former. Distortions from a regular geometry can be ascribed in part to the restricted bite distances of the xanthate ligands, which form the most acute angles. The widest angle subtended at the zinc atom involves the two weakly bound sulphur atoms.

The main feature of the molecular packing of **I** is the formation of dimeric (centrosymmetric) aggregates mediated by hmta-methylene-C–H···N(hmta) interactions which are connected into a supramolecular chain along the b-axis by S1···S1 contacts, Figure 3a; Table 3 collates the geometric characteristics of the major intermolecular interactions operating in the crystal structures of **I–IV**. The chains pack in layers but with no directional interactions within or between layers according to the standard distance criteria assumed in PLATON [19], Figure 3b.

The molecular structure of [Zn(S₂CO-iPr)₂(hmta)], (**II**), Figure 4 and Table 2, exhibits similar characteristics as
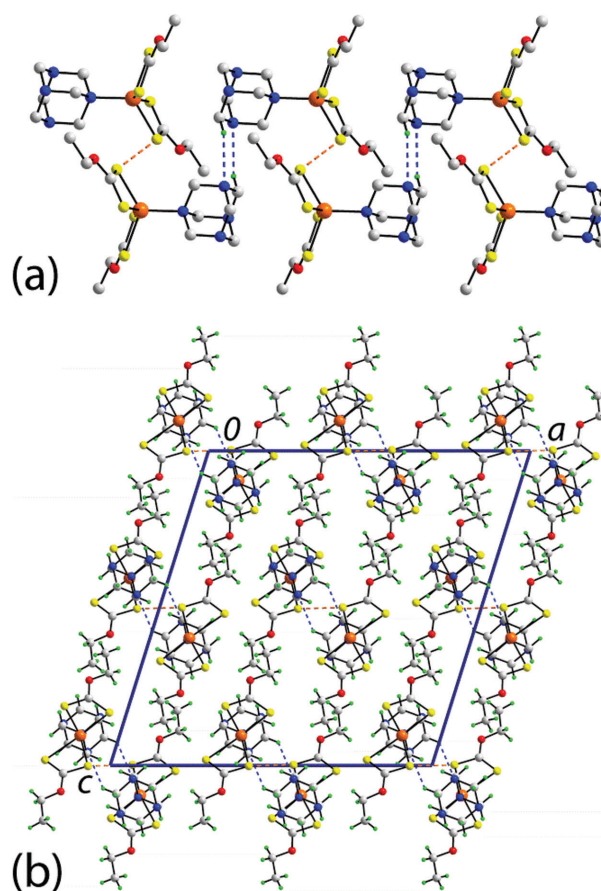
Fig. 3: Molecular packing in **I**: (a) supramolecular chain along the b-axis sustained by hmta-methylene-C–H···N(hmta) and S1···S1 interactions (non-interacting hydrogen atoms have been removed), and (b) view in projection down the b-axis of the unit cell contents. The C–H···N and C–H···N interactions are shown as blue- and orange-dashed lines, respectively.

Tab. 3: Summary of intermolecular interactions (A–H···B; Å, °) operating in the crystal structures of **I–IV**.

A	H	B	A–H	H···B	A···B	A–H···B	Symmetry operation
I							
C11	H11b	N2	0.99	2.60	3.326(8)	130	$1-x, 2-y, -z$
S1	–	S1	–	–	3.237(3)	–	$1-x, 1-y, -z$
II							
C11	H11b	O1	0.99	2.44	3.379(3)	158	$\frac{1}{2}-x, -\frac{1}{2}+y, 1\frac{1}{2}-z$
III							
C4	H4b	N2	0.99	2.58	3.521(4)	160	$x, -1+y, z$
C16	H16b	Cg(Zn,S3,S4,C6)	0.99	2.94	3.911(3)	168	$-1+x, y, z$
S4	–	S4	–	–	3.3177(10)	–	$1-x, 2-y, 1-z$
IV							
O1a	H1o	O2b	0.85(2)	1.90(2)	2.743(3)	179(4)	$-x, 1-y, 1-z$
O2a	H2o	O2c	0.832(19)	1.929(19)	2.760(3)	177(2)	$1+x, -1+y, 1+z$
O1b	H3o	N6d	0.834(16)	1.980(18)	2.790(3)	164(4)	$1-x, 1-y, 1-z$
O2b	H4o	S3c	0.84(3)	2.54(3)	3.316(3)	153(3)	x, y, z
O1c	H5o	O1d	0.84(2)	1.88(2)	2.673(3)	158(3)	$2-x, 1-y, 1-z$
O2c	H6o	S1a	0.837(16)	2.69(2)	3.448(2)	152(2)	$-x, 1-y, 1-z$
O1d	H7o	N5b	0.834(14)	1.947(17)	2.769(3)	168(4)	$1-x, 1-y, 1-z$
O2d	H8o	O1b	0.84(3)	2.04(3)	2.667(3)	131(3)	$x, 1+y, z$
C16c	H16f	O1a	0.99	2.58	3.488(3)	152	$x, y, -1+z$
C17c	H17e	O1a	0.99	2.58	3.485(3)	152	$x, y, -1+z$
C17d	H17i	N6a	0.99	2.57	3.491(4)	154	$x, 1+y, z$
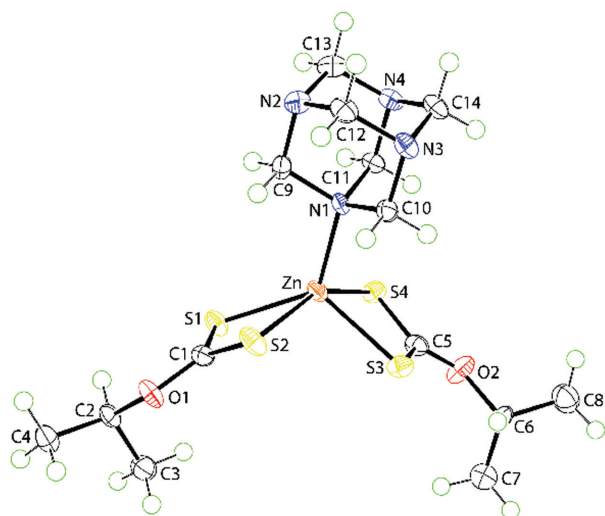
Fig. 4: The molecular structure of **II**, showing atom-labelling and displacements ellipsoids at the 50% probability level.

described for **I**. The value of ΔS for the S1-xanthate ligand is 0.57 Å, considerably greater than 0.10 Å for the S3-xanthate. The greater precision in the analysis of **II** enables a correlation of the Zn–S bond lengths with the associated C–S bonds. Thus, for the S1-xanthate ligand, the disparity in the Zn–S1, S2 bonds correlates with the difference in the C1–S1, S2 bond lengths with C1–S1, involving the more tightly bound S1 atom, being considerably longer than the C1–S2 bond, Table 2. This disparity is no longer evident

in C5–S3, S4 when the differences in the Zn–S3, S4 bond lengths is much smaller so that C5–S3 is only marginally longer than C5–S4. The NS$_4$ donor set defines an intermediate geometry between square pyramidal and trigonal bipyramidal. However, by contrast to the situation for **I**, the calculated value of τ [22], i.e. 0.58, suggests a distortion towards the latter.

In the molecular packing of **II**, molecules self-assemble into a supramolecular chain along the b-axis with a helical topology (2$_1$-screw axis) being connected by methylene-C–H···O interactions, Figure 5(a) and Table 3. Reinforcing these chains are secondary Zn···S2^i interactions of 3.8724(7) Å cf. 4.05 Å, being the sum of the van der Waals radii of Zn and S [23]; symmetry operation i: ½–x, −½+y, 1½–z. The chains assemble in the ab-plane with no specific interactions between them and similarly interdigitate along the c-axis without contacts, judged on the normal distance criteria [19], Figure 5(b).

Attention is now directed towards the dithiocarbamate analogues of **I** and **II**: the molecular structure of [Zn(S$_2$CNEt$_2$)$_2$(hmta)], (**III**), Figure 6 and Table 3, is, to a first approximation, similar to the xanthate structures. Thus, the zinc(II) centre is chelated by two dithiocarbamate ligands and the penta-coordinated geometry is completed by a hmta ligand coordinating in the monodentate mode. The S1-containing dithiocarbamate ligand forms Zn–S1, S2 bonds with ΔS = 0.30 Å, a value greater than ΔS = 0.16 Å formed by the S3-dithiocarbamate. For the
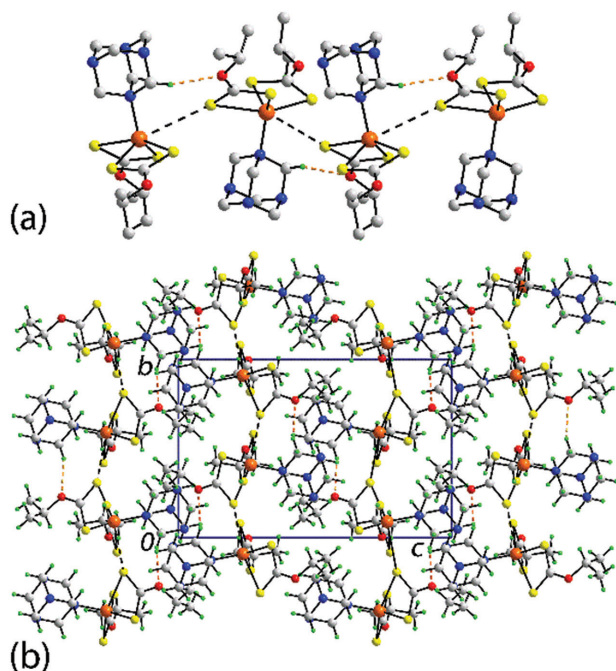
Fig. 5: Molecular packing in **II**: (a) supramolecular chain along the b-axis sustained by C−H···N and Zn···S interactions (non-interacting hydrogen atoms have been removed), and (b) view in projection down the a-axis of the unit cell contents. The C−H···N and Zn···S interactions are shown as blue- and black-dashed lines, respectively.
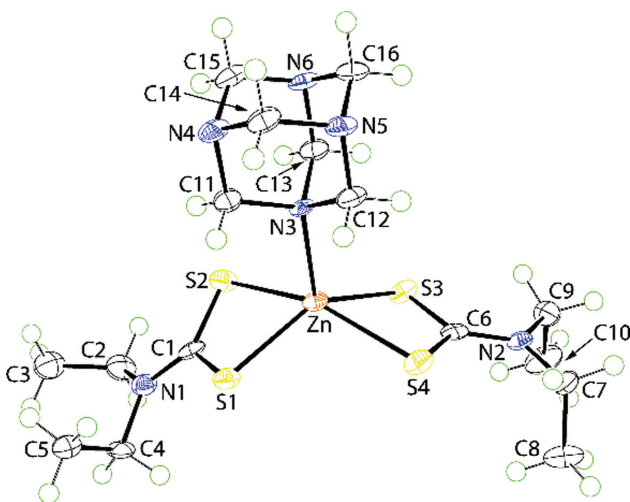

Fig. 6: The molecular structure of **III,** showing atom-labelling and displacements ellipsoids at the 70% probability level.

asymmetrically coordinating ligand, the disparity in the Zn−S1, S2 bond lengths is reflected in the associated C−S1, S2 bonds whereas for the more symmetrically coordinating ligand, the C−S3, S4 bond lengths are equal within experimental error. The value of τ computes to 0.33,

indicating a coordination geometry skewed towards a square pyramid. Similar trends in the bond angles as for the xanthate structures are apparent, Table 4.

Globally, the molecular packing of **III** may be described as comprising double layers of molecules that stack along the c-axis with no directional interactions between them. Supramolecular layers in the ab-plane are sustained by dithiocarbamate-methylene-C−H···N(hmta) and C−H···π interactions between hmta-C−H and where the π-system is defined by the ZnS_2C chelate ring, Figure 7a. Similar C−H···π(chelate ring) interactions are now well known in the supramolecular chemistry of metal 1,1-dithiolates, including xanthates and dithiocarbamates [12, 25−29], as well as in other systems such as metal acetylacetonates [30]. Centrosymmetrically layers are linked via S4···S4[i] interactions of 3.3177(10) Å, cf. the sum of the van der Waals radii = 3.60 Å [23]; symmetry operation i: 1−*x*, 2−*y*, 1−*z*, and the resultant double layers assemble along the c-axis being separated by hydrophobic interactions, Figure 7(b).

The final structure to be discussed, i.e. **IV**, contains dithiocarbamate ligands functionalised with hydrogen bonding potential, Figure 8 and Table 3. A notable feature of the structure is the presence of four independent molecules in the crystallographic asymmetric unit. A recent survey showed metal-containing molecules exhibited Z′ > 1 in 9.2% in their structures cf. 12.3% for all-organic molecules [31]. These numbers rise for triclinic space groups based on an earlier survey of 173,479 non-polymeric structures comprising one chemical species only [32]. Thus, Z′ > 1 occurs in 15.6 and 22.6% of triclinic metalorganic and all-organic crystal structures, respectively. Just 0.69% of structures in this survey featured the $P\bar{1}$ space group with four independent molecules in the asymmetric unit [32].

As for the structures above, the zinc atom in each independent molecule is chelated by two 1,1-dithiolate ligands and coordinated by the monodentate hmta ligand. There are distinguishing features in the molecular structures, starting from the modes of coordination of the dithiocarbamate ligands. The pattern in ΔS for **III**, i.e. one ligand forming more asymmetric bonds than the other, is followed for molecules a, b and d, but both ligands are coordinating similarly in molecule c with ΔS being 0.27 and 0.28 Å, i.e. intermediate cf. the ΔS values for the remaining structures which range from 0.19 Å for the S3-dithiocarbamate ligand in molecule d to 0.38 for the S1-dithiocarbamate in b. As for **III**, as a general principle, the C−S bond lengths associated more asymmetrically coordinating ligands are experimentally distinct. While spanning a range, the τ values of 0.38, 0.45, 0.38 and 0.23 for a−d, respectively, indicate distortions in the coordination geometries towards square

Tab. 4: Selected geometric parameters (Å, °) for **III** and **IV**.

|	III (n = 6)	IV (n = 7) molecule a	IV (n = 7) molecule b	IV (n = 7) molecule c	IV (n = 7) molecule d
Zn–S1	2.3358(7)	2.3432(7)	2.3132(7)	2.3388(7)	2.3261(7)
Zn–S2	2.6525(8)	2.6657(7)	2.6890(7)	2.6084(7)	2.6748(7)
Zn–S3	2.3671(7)	2.3452(7)	2.3435(7)	2.3441(7)	2.3498(7)
Zn–S4	2.5312(8)	2.5699(7)	2.5436(7)	2.6197(7)	2.5365(8)
Zn–N3	2.102(2)	2.091(2)	2.114(2)	2.087(2)	2.108(2)
C1–S1	1.741(3)	1.744(3)	1.737(3)	1.737(3)	1.735(3)
C1–S2	1.715(3)	1.718(3)	1.719(3)	1.713(3)	1.723(3)
C1–N1	1.331(3)	1.335(3)	1.338(3)	1.338(3)	1.332(3)
C(n)–S3	1.723(3)	1.737(3)	1.736(3)	1.746(3)	1.732(3)
C(n)–S4	1.723(3)	1.718(3)	1.721(3)	1.717(3)	1.718(3)
C(n)–N2	1.338(3)	1.334(3)	1.330(3)	1.332(3)	1.333(3)
S1–Hg–S2	72.40(2)	71.91(2)	72.22(2)	73.03(2)	72.26(2)
S1–Hg–S3	137.56(3)	137.06(3)	137.24(3)	137.88(3)	143.93(3)
S1–Hg–S4	101.99(2)	101.62(2)	106.79(3)	103.63(2)	102.69(3)
S1–Hg–N3	111.48(6)	113.39(6)	113.01(6)	108.82(6)	110.83(6)
S2–Hg–S3	95.16(2)	97.95(2)	95.85(2)	96.80(2)	97.07(2)
S2–Hg–S4	157.22(3)	160.14(3)	164.39(3)	160.67(3)	157.80(3)
S2–Hg–N3	96.75(6)	97.64(6)	94.41(6)	104.71(6)	94.87(6)
S3–Hg–S4	73.85(2)	73.68(2)	74.13(2)	72.62(2)	74.06(2)
S3–Hg–N3	110.19(6)	109.25(6)	108.67(6)	113.29(6)	104.24(6)
S4–Hg–N3	105.73(6)	102.12(6)	100.11(6)	94.43(6)	106.96(6)
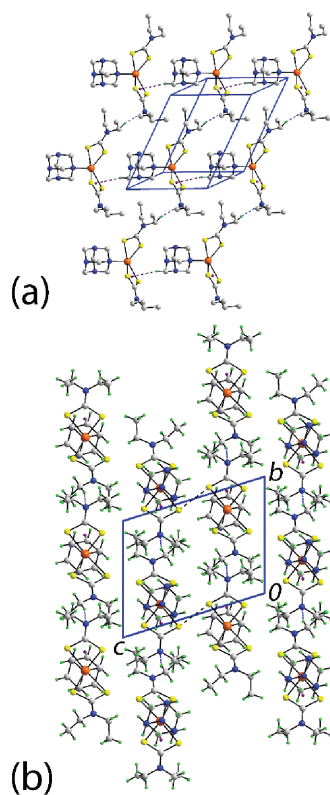
Fig. 7: Molecular packing in **III**: (a) supramolecular layer in the ab-plane sustained by C–H···N and C–H···π(chelate) interactions (non-interacting hydrogen atoms have been removed), and (b) view in projection down the a-axis of the unit cell contents highlighting the S···S leading to double-layers. The C–H···N, C–H···π(chelate) and S···S interactions are shown as blue-, purple and black-dashed lines, respectively.

pyramidal. As gleaned from the diagrams in Figure 8, the dithiocarbamate ligands overlap to a first approximation being related by a non-crystallographic two-fold rotation aligned along the Zn–N bond. Conformational differences are apparent in the relative orientations of the N-bound hydroxyethyl and isopropyl substituents. More notable is the disparity in the relative orientations of the hmta ligands with respect to the ZnS_4 chromophore in the four molecules. This is not to imply different conformations of the hmta ligands as an overlay diagram of the four independent molecules (not shown) confirm that are strictly superimposable and have the same all-chair conformation found in the structure of the well-studied, uncoordinated hmta molecule but lacking the high symmetry [1, 33, 34].

With eight independent hydroxyl groups, substantial hydrogen bonding is anticipated in the molecular packing. Indeed, each hydroxyl group participates in a donor interaction. While this is true, there are only four hydroxyl-O–H···O(hydroxyl) hydrogen bonds and these are complimented by two hydroxyl-O–H···S(dithiocarbamate) and two hydroxyl-O–H···N(hmta) hydrogen bonds, Table 4. Although the formation of other than hydroxyl-O–H···O(hydroxyl) hydrogen bonds maybe unexpected, this is often observed in the supramolecular chemistry of hydroxyethyl-substituted dithiocarbamate compounds [10, 35–37]. Also surprising is that despite the large number of hydrogen bonds, these sustain a supramolecular layer parallel to (0 1 4), Figure 9a, rather than a three-dimensional architecture. The Zn1-Zn4-containing molecules interact via hydrogen bonds with three (via O–H···O
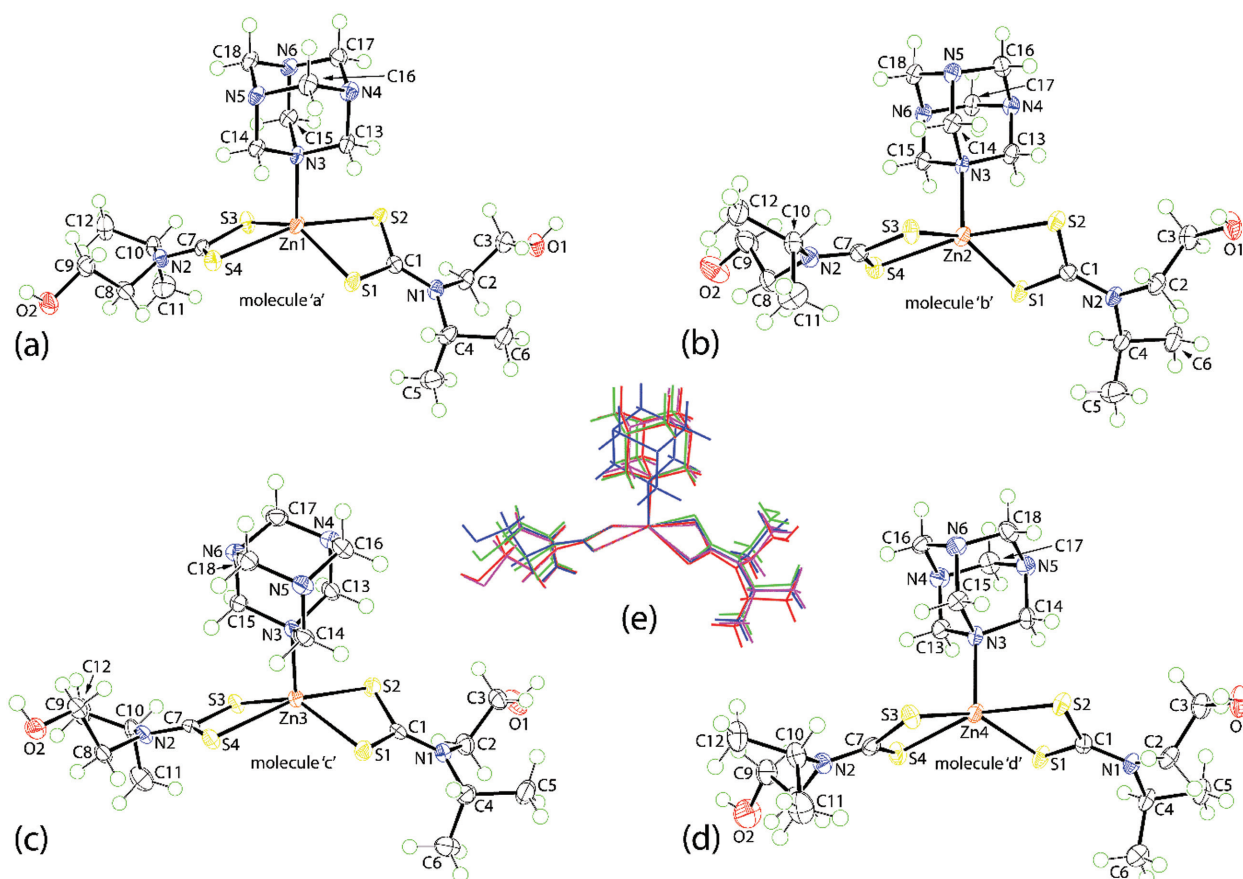
Fig. 8: The molecular structures comprising the asymmetric unit of **IV**, showing atom-labelling and displacements ellipsoids at the 70% probability level: (a) molecule a, (b) molecule b, (c) molecule c and (d) molecule d {the C8 atom is obscured}. (e) Overlay diagram for molecules a (red image), b (inverted molecule, green), c (blue) and d (inverted molecule, pink). The molecules have been overlapped so that the Zn, S3, S4, C7 chelate rings are superimposed.

(x2) and S···H–O), four (O–H···N, O–H···S, O···H–O and N···H–O), four (O–H···O, O–H···S, O···H–O and S···H-O) and four (O–H···O, O–H···N, O···H–O and N···H–O) molecules, respectively, which exist in well-defined domains as illustrated in Figure 9b; the diversity in hydrogen bond formation further differentiates the four independent molecules. Layers thus formed are connected via hmta-methylene-C–H···O, N interactions, Figure 9c and Table 3.

Discussion

The common feature of the four structures reported herein is the adoption of penta-coordinate geometries defined by two chelating 1,1-dithiolate ligands and monodentate hmta ligands. Generally, one 1,1-dithiolate ligand chelates with considerably more asymmetry than the other. The resulting NS$_4$ donor sets define heavily distorted geometries being intermediate between trigonal bipyramidal

and square pyramidal with general tendencies towards the latter. Differences between **I** and **II** on the one the one hand and **III** and **IV** on the other are related to the nature of the 1,1-dithiolate ligands. Referring to Figure 10, the contribution of the canonical forms to the overall electronic structures of the xanthate and dithiocarbamate anions are about 20 and 40%, respectively [25, 38, 39]. This has the consequence that the dithiocarbamate ligand is a more effective chelating agent explaining the more symmetric coordination modes in **III** and **IV**. The systematic elongation of the Zn–N bond lengths in **III** and **IV**, Table 4 cf. those in **I** and **II**, Table 2, is therefore explained. Finally, the appearance of the stand-alone intermolecular C–H···π(chelate) interaction in **III**, involving the more symmetrically coordinating dithiocarbamate ligand, is consistent with greater metalloaromatic character [40–42]. It is noted that non-aromatic systems may also form analogous interactions [43–45].

As indicated in the Introduction, analogous chemistry between cadmium xanthates and hmta was explored
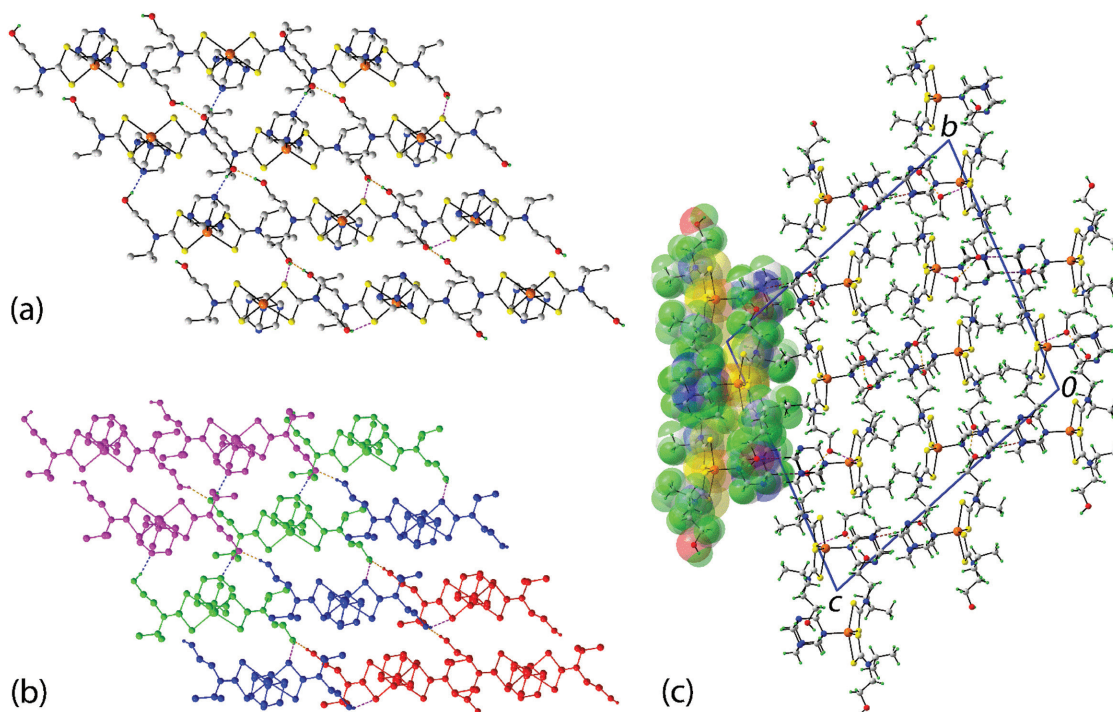
Fig. 9: Molecular packing in **IV**: (a) supramolecular layer parallel to (0 1 4) sustained by O−H···O, O−H···N and O−H···S hydrogen bonding (non-interacting hydrogen atoms have been removed), (b) view highlighting the different molecules comprising the asymmetric unit: molecule a is shown in red, b in green, c in blue and d in pink, and (c) view in projection down the a-axis of the unit cell contents highlighting the C−H···O and C−H···N connections between layers. One layer is highlighted in space-filling mode. The O−H···O, O−H···N, O−H···S, C−H···O and C−H···N interactions are shown as orange-, blue-, pink-, purple- and brown-dashed lines, respectively.
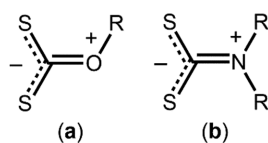

Fig. 10: Promient canonical structures for (**a**) xanthate and (**b**) dithiocarbamate anions.

recently [10]. By contrast to the 1:1 adducts formed herein, depending on the size of R in $Cd(S_2COR)_2$, different ratios of $Cd(S_2COR)_2$ and hmta were formed in the adducts $Cd(S_2COMe)_2(hmta)$, $Cd(S_2COEt)_2(hmta)_{0.5}$ and $Cd(S_2COiPr)_2(hmta)$, regardless of the ratios (1:2, 1:1 and 2:1) of the reagents in the reaction medium. While such an extensive study was not performed herein, only 1:1 species were isolated in the case of $Zn(S_2COEt)_2$ when reacted with 0.5 or 2 molar equivalents of hmta.

There are literature precedents for **III** whereby **III** has been isolated as a co-crystal with fullerene (C_{60}) with chlorobenzene as the occluded solvent; the ratio of the species is 2:1:1 [46]. Figure 11 shows an overlay diagram of **III** with the two molecules from the literature and several conformational differences are evident. It is suggested that the differences between the molecules relate to the formation
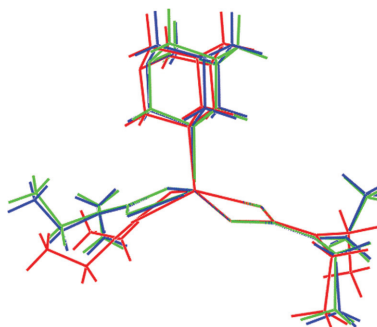

Fig. 11: Overlay diagram for molecules of **III** (red image), literature molecules 1 (green) and 2 (inverted molecule, blue). Each of the molecules has been overlapped so that the most symmetric chelate ring is coincident.

of the aforementioned C−H···π(chelate ring) interaction in the molecular packing of **III**. Thus, the ΔS values for the Zn1- and Zn2-containing literature molecules of 0.23 and 0.28 Å, and 0.21 and 0.30 Å, respectively, are to a first approximation intermediate between those of **III**, i.e. 0.16 and 0.30 Å; the more symmetric ring in **III** is the π-system in the C−H···π(chelate ring) contact. Also, to enable this contact, the ethyl groups of the dithiocarbamate ring must be directed towards the same side of the ligand; all

other conformations have the rings lying to either side, Figure 10, as is normally observed for diethyldithiocarbamate ligands [39, 40]. Compared to the literature molecules, the second dithiocarbamate and hmta ligands are pushed away from the symmetric dithiocarbamate ligand, again due to the close approach of a symmetry related hmta molecule to enable the C–H···π(chelate ring) contact. Finally, the τ values of 0.25 and 0.28, cf. 0.33 for literature **III**, indicate greater distortions towards square pyramidal geometries.

By contrast to xanthate and dithiocarbamate ligands, equivalent canonical structures to those shown in Figure 10 do not exist for the dithiophosphate, $^-[S_2P(OR)_2]$, and dithiophosphinateand, $^-S_2PR_2$, ligands owing to the tetrahedral geometry of the phosphorus atom. Accordingly, these ligands are less likely to be chelating and show a greater propensity for bridging metal centres [7, 8, 47, 48], often via secondary interactions [49, 50], and therefore, to form coordination polymers with polyfunctional Lewis base donors [51, 52]. In this context, all of the known metal dithiophosphates/dithiophosphinates adducts of hmta bar one, have the latter coordinating in a bidentate, bridging mode [53–55]. The exceptional structure is that of $Cd[S_2P(OEt)_2]_2(hmta)_2$ with monodentate hmta ligands [56].

Conclusions

The polyfunctional hmta ligand functions as a monodentate ligand to binary zinc(II) xanthates (**I** and **II**) and dithiocarbamates (**III** and **IV**), leading to NS_4 donor sets which define distorted coordination geometries tending towards square pyramidal. Systematic variations between the xanthate and dithiocarbamate structures are correlated with the enhanced coordinating ability of the latter. As expected from the composition, the three-dimensional molecular packing in **IV** is sustained by hydrogen bonding. By contrast, weaker interactions contribute to the stabilisation of the crystal structures of **I**–**III**. Of interest is the formation of a C–H···π(chelate ring) interaction in **III**, a result correlated with the greater chelating ability of the dithiocarbamate ligand involved in forming this contact, a contact that is of sufficient strength to influence the relative orientation of the other components of the molecule.

References

[1] R. G. Dickinson, A. L. Raymond, *J. Am. Chem. Soc.* **1923**, *45*, 22.
[2] S.-L. Zheng, M.-L. Teng, X.-M. Chen, *Coord. Chem. Rev.* **2003**, *246*, 185.
[3] J. J. Perry, J. A. Perman, M. J. Zaworotko, *Chem. Soc. Rev.* **2009**, *38*, 140.
[4] A. M. Kirillov, *Coord. Chem. Rev.* **2011**, *255*, 1603.
[5] C. R. Groom, I. J. Bruno, M. P. Lightfoot, S. C. Ward, *Acta Crystallogr. B* **2016**, *72*, 171.
[6] Y. S. Tan, A. D. Azizuddin, M. V. Câmpian, I. Haiduc, E. R. T. Tiekink, *Z. Kristallogr.* **2016**, *231*, 155.
[7] E. R. T. Tiekink, *CrystEngComm* **2003**, *5*, 101.
[8] E. R. T. Tiekink, *CrystEngComm* **2006**, *8*, 104.
[9] Y. S. Tan, A. L. Sudlow, K. C. Molloy, Y. Morishima, K. Fujisawa, W. J. Jackson, W. Henderson, S. N. Bt. A. Halim, S. W. Ng, E. R. T. Tiekink, *Cryst. Growth Des.* **2013**, *13*, 3046.
[10] Y. S. Tan, S. N. A. Halim, E. R. T. Tiekink, *Z. Kristallogr.* **2016**, *231*, 113.
[11] S. A. M. Safbri, S. N. A. Halim, M. M. Jotani, E. R. T. Tiekink, *Acta Crystallogr. E* **2016**, *72*, 158.
[12] M. M. Jotani, Y. S. Tan, E. R. T. Tiekink, *Z. Kristallogr.* **2016**, *231*, 403.
[13] *CrystalClear*. User Manual. Rigaku/MSC Inc., Rigaku Corporation, The Woodlands, TX, **2005**.
[14] T. Higashi, *ABSCOR*. Rigaku Corporation, Tokyo, Japan, **1995**.
[15] Agilent Technologies, *CrysAlisPro*. Santa Clara, CA, USA. **2014**.
[16] G. M. Sheldrick, *Acta Crystallogr. Sect. A, Foundat. Crystallogr.* **2008**, *64*, 112.
[17] G. M. Sheldrick, *Acta Crystallogr. Sect. C, Cryst. Struct Commun.* **2015**, *71*, 3.
[18] L. J. Farrugia, *J. Appl. Crystallogr.* **2012**, *45*, 849.
[19] A. L. Spek, *Acta Crystallogr. Sect. D, Biol. Crystallogr.* **2009**, *65*, 148.
[20] *DIAMOND, Visual Crystal Structure Information System, Version 3.1*, CRYSTAL IMPACT, Postfach 1251, D-53002 Bonn, Germany, **2006**.
[21] J. Gans, D. Shalloway, *J. Mol. Graph. Model.* **2001**, *19*, 557.
[22] A. W. Addison, T. N. Rao, J. Reedijk, J. van Rijn, G. C. Verschoor, *J. Chem. Soc. Dalton Trans.* **1984**, 1349.
[23] A. Bondi, *J. Phys. Chem*. **1964**, *68*, 441.
[24] D. Chen, C. S. Lai, E. R. T. Tiekink, *Z. Kristallogr.* **2003**, *218*, 747.
[25] E. R. T. Tiekink, I. Haiduc, *Prog. Inorg. Chem*. **2005**, *54*, 127.
[26] E. R. T. Tiekink, J. Zukerman-Schpector, *Chem. Commun.* **2011**, *47*, 6623.
[27] J. Zukerman-Schpector, E. R. T. Tiekink, in *The Importance of Pi-Interactions in Crystal Engineering – Frontiers in Crystal Engineering*, (Eds. E. R. T. Tiekink, J. Zukerman-Schpector) John Wiley & Sons Ltd, Singapore, pp. 275, **2012**.
[28] A. N. Gupta, V. Kumar, V. Singh, K. K. Manar, M. G. B. Drew, N. Singh, *CrystEngComm* **2014**, *16*, 9299.
[29] Y. S. Tan, S. N. A. Halim, K. C. Molloy, A. L. Sudlow, A. Otero-de-la-Roza, E. R. T. Tiekink, *CrystEngComm* **2016**, *18*, 1105.
[30] M. K. Milčič, V. B. Medaković, D. N. Sredojević, N. O. Juranić, Z. D. Tomić and S. D. Zarić, *Inorg. Chem*. **2006**, *45*, 4755.

Q3: Please supply volume number for Ref. [22]

Q4: Ref. [24] is not cited in text. Please supply text citation or delete the references from the references list

[31] K. M. Steed, J. W. Steed, *Chem. Rev.* **2015**, *115*, 2895.

[32] A. D. Bond, *CrystEngComm* **2008**, *10*, 411.

[33] L. N. Becka, D. W. J. Cruickshank, *Proc. R. Soc. London, Ser. A* **1963**, *273*, 435.

[34] S. P. Kampermann, T. M. Sabine, B. M. Craven, R. K. McMullan Acta Crystallogr. A **1995**, *51*, 489.

[35] R. A. Howie, G. M. de Lima, D. C. Menezes, J. L. Wardell, S. M. S. V. Wardell, D. J. Young, E. R. T. Tiekink, *CrystEngComm* **2008**, *10*, 1626.

[36] N. S. Jamaludin, Z.-J. Goh, Y. K. Cheah, K.-P. Ang, J. H. Sim, C. H. Khoo, Z. A. Fairuz, S. N. B. A. Halim, S. W. Ng, H.-L. Seng, E. R. T. Tiekink, *Eur. J. Med. Chem.* **2013**, *67*, 127.

[37] N. S. Jamaludin, S. N. B. A. Halim, C.-H. Khoo, B.-J. Chen, T.-H. See, J.-H. Sim, Y.-K. Cheah, H.-L. Seng, E. R. T. Tiekink, *Z. Kristallogr.* **2016**, *231*, 341.

[38] P. J. Heard, *Prog. Inorg. Chem.* **2005**, *53*, 1.

[39] G. Hogarth, *Prog. Inorg. Chem.* **2005**, *53*, 71.

[40] H. Masui, *Coord. Chem. Rev.* **2001**, *219–221*, 957.

[41] Y. Z. Wang, G. H. Robinson, *Organometallics* **2007**, *26*, 2.

[42] M. K. Milčić, B. D. Ostojić, S. D. Zarić, *Inorg. Chem.* **2007**, *46*, 7109.

[43] S. E. Wheeler, *Acc. Chem. Res.* **2013**, *46*, 1029.

[44] C. I. Yeo, S. N. A. Halim, S. W. Ng, S. L. Tan, J. Zukerman-Schpector, M. A. B. Ferreira, E. R. T. Tiekink, *Chem. Commun.* **2014**, *50*, 5984.

[45] J. Zukerman-Schpector, C. I. Yeo, E. R. T. Tiekink, *Z. Kristallogr.* **2016**, *231*, 55.

[46] D. V. Konarev, S. S. Khasanov, A. Yu. Kovalevsky, D. V. Lopatin, V. V. Rodaev, G. Saito, B. Náfrádi, L. Forró, R. N. Lyubovskaya, *Cryst. Growth Des.* **2008**, *8*, 1161.

[47] I. Haiduc, D. B. Sowerby, *Polyhedron* **1996**, *15*, 2469.

[48] I. Haiduc, 1,1-Dithiolato Ligands, in vol. *Comprehensive Coordination Chemistry II. From Biology to Nanotechnology*, J. A. McCleverty, T. J. Meyer, Editors-in-Chief, Volume 1, Fundamentals, (Ed. A. B. P. Lever) Elsevier, Chapter 1.15, p. 349, **2003**.

[49] N. W. Alcock, *Adv. Inorg. Chem. Radiochem.*, **1972**, *15*, 1.

[50] I. Haiduc, *Secondary Bonding* in J. L. Atwood and J. Steed (Eds), *Encyclopedia of Supramolecular Chemistry*, Marcel Dekker Inc., New York, **2004**, 1215.

[51] C. S. Lai, S. Liu, E. R. T. Tiekink, *CrystEngComm* **2004**, *6*, 221.

[52] C. S. Lai, S. Liu, E. R. T. Tiekink, *CrystEngComm* **2004**, *6*, 593.

[53] L. Bolundut, I. Haiduc, M. F. Mahon, K. C. Molloy, *Rev. Chim. (Bucharest Rom.)* **2008**, *59*, 1194.

[54] T. E. Kokina, R. F. Klevtsova, L. A. Glinskaya, S. V. Larionov, *Russ. J. Inorg. Chem.* **2010**, *55*, 56.

[55] S. V. Larionov, T. E. Kokina, L. A. Glinskaya, R. F. Klevtsova, *Russ. J. Coord. Chem.* **2002**, *28*, 560.

[56] M. Shimoi, A. Ouchi, M. Aikawa, S. Satoa, Y. Saito, *Bull. Chem. Soc. Jpn.* **1982**, *55*, 2089.

Graphical synopsis

Marius V. Câmpian, Aliaa Diyana Azizuddin, Ionel Haiduc and Edward R.T. Tiekink

Mono urotropine adducts of some binary zinc xanthates and dithiocarbamates: solid-state molecular structures and supramolecular self-assembly

Synopsis: Urotropine forms 1:1 adducts with zinc xanthates and zinc dithiocarbamates.